AIR-BRIDGE CELLS FOR HIGHER EMISSION TEMPERATURES

Bosun Roy-Layinde, Areefa Rahman, Jihun Lim, Sritoma Paul, Stephen R. Forrest and Andrej Lenert

University of Michigan, Ann Arbor, Michigan, USA

***Abstract* — Interest in thermal batteries for inexpensive grid-scale storage of renewable energy motivates the development of photovoltaics that efficiently convert very high temperature thermal emission to electrical energy. We have previously shown that InGaAs air-bridge cells can increase TPV efficiency by ~30% compared to cells with more conventional back surface reflectors. In this study, we design and experimentally characterize airbridge cells with wider bandgaps for applications at higher emission temperatures. Parametric studies with varying bandgap and emitter temperature identify high performance regimes. At temperatures up to 2000K, predicted device efficiencies of single-junction air-bridge cells match that of record-holding multi-junction cells. Furthermore, a novel platform for device testing using porous graphite emitters is designed and experimentally demonstrated.**

I. Introduction

Thermophotovoltaic (TPV) conversion of thermal radiation to electrical power is a readily scalable process for on-demand electricity generation. A TPV system consists of two major parts, a thermal emitter and a photovoltaic cell in close proximity, as shown in Fig. 1a. Heat supplied by an upstream primary energy source maintains the emitter at elevated temperatures (>1000 K) which drives emission of infrared radiation. Photons with energy greater than its bandgap (in-band) excite electron-hole pairs. Meanwhile, absorption of emitted photons with energy less than the bandgap (out-of-band) generates undesirable low-grade waste heat.

TPVs can be used for a broad range of applications, which include waste heat recovery (800-1300 K), direct solar thermal energy conversion (1000-1300 K), space exploration (1200-1400 K), cogeneration of heat and power (1300-1500 K), and grid scale thermal storage (1500-2400 K) [1]–[4]. However, current approaches to TPV generation are typically optimized for a specific temperature range and do not translate easily to other temperatures and applications.

In our prior work, we demonstrated a record high 98.5% out-of-band reflectance R_{out} enabled by an air cavity situated between the absorber and reflector [5]. This airbridge cell improved the TPV efficiency by 25-30% compared to a cell without the air cavity.

The objective of this work is to identify a set of cell designs, all within one material system, that enable highly efficient conversion across a very wide range of blackbody emission temperatures and that are specifically suitable for energy storage applications. To this end, we design airbridge cells (ABCs) within the $In_{1-x}Ga_xAs_{1-y}P_y$ (InGaAsP) material system, which is lattice-matched to InP substrates. The binary materials for this quaternary system include GaP, GaAs, InAs and InP. These four materials play a role in determining the material properties for the InGaAsP quaternary cell by compositional mixing. Fig. 1b shows the bandgap energy as a function of lattice constants where the red dashed line indicates the bandgap range when lattice matched to InP. The bandgap range is wide, from 0.74 eV to 1.35 eV, which makes it possible to match the bandgap to different emission temperatures.

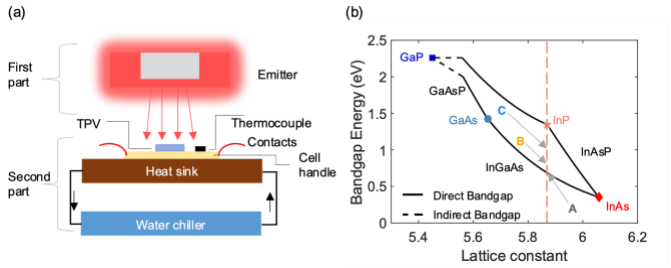

Fig. 1 (a) Thermophotovoltaic system consisting of the heat source (emitter) and the cold source (photovoltaic cell). **(b)** Bandgap diagram as a function of lattice constant for binary and ternary III-V semiconductors.

II. Theory and Design

The conversion efficiency η of a TPV system is defined as the ratio of the electrical power output P_{mpp} to the heat absorbed by the cell Q_{abs}. Absorption of out-of-band photons ($E<E_g$) represents one of the greatest losses. Therefore, TPV systems must realize wavelength-selective radiative transfer between the emitter and cell to achieve high efficiencies. One method for achieving selectivity is photon recuperation, a process by which low energy photons are reflected back to the emitter are reabsorbed [5]–[7]. The other common approach involves the use of selective emitters that preferentially emit in-band photons [8]. The TPV conversion efficiency also depends on the cell's ability to collect photoexcited charge carriers. Aligning the bandgap to the emission spectrum to ensure proper photon utilization is another major design consideration in improving device performance. Other major losses in the device include resistive (ohmic) losses and non-radiative recombination.

To understand the different factors that contribute to efficiency, we can decouple the conversion efficiency into the product of two meaningful performance metrics [8], namely spectral management $(SE)(IQE)$ and carrier management $(VF)(FF)$ efficiencies, as given by:

$$\eta = \left(\frac{P_{mpp}}{Q_{abs}}\right) = (SE)(IQE)(VF)(FF) \qquad (1)$$

In this work, we model the electronic and optical properties of the quaternary InGaAsP/InP heterojunction for the three

different systems. To achieve bandgaps of 0.74 eV, 1.0 eV and 1.2 eV, we use alloy compositions of $In_{0.53}Ga_{0.47}As_1P_0$, $In_{0.76}Ga_{0.24}As_{0.52}P_{0.48}$ and $In_{0.9}Ga_{0.1}As_{0.21}P_{0.79}$ respectively, as determined by equation 2 [9].

$$M = x \cdot y \cdot B_{GaP} + x \cdot (1-y) \cdot B_{GaAs} + (1-x) \cdot y \cdot B_{InP} + (1-x) \cdot (1-y) \cdot B_{InAs} \quad (2)$$

The absorption coefficients (α) for the cells were modeled using a piece-wise function (from [10]), given by:

$$\alpha = \begin{cases} \alpha_0 \exp\left(\frac{E - E_g}{E_0}\right), E \le E_g \\ \alpha_0 \exp\left(1 + \frac{E - E_g}{E'}\right), E \ge E_g \end{cases} \quad (3)$$

These coefficients were fed into a transfer matrix model that resolves the electric field distribution inside the cell.

The electronic properties (current-voltage characteristics) are modeled as in our prior work using a two-diode model [11] [12], which describes different rates of recombination in the depleted and quasi-neutral regions. This model assumes the cell has a series resistance of 30 $m\Omega.cm^2$ and is being cooled to a constant cell temperature of 298 K.

III. Results and Discussion

To understand how charge collection differs for the three systems, we plot (*VF*)(*FF*) as a function of increasing temperature as shown in Fig. 2a. Larger bandgaps produce better (*VF*)(*FF*) at higher emitter temperatures. At relatively low temperatures (< 1000 K), the three different systems have comparable (*VF*)(*FF*). As the temperature increases, we see a common trend where (*VF*)(*FF*) increases until a maximum point where further increase in heat source temperature leads to a reduction in performance. The eventual decline in (*VF*)(*FF*) is due to resistive losses which scale quadratically with the increasing photocurrent density.

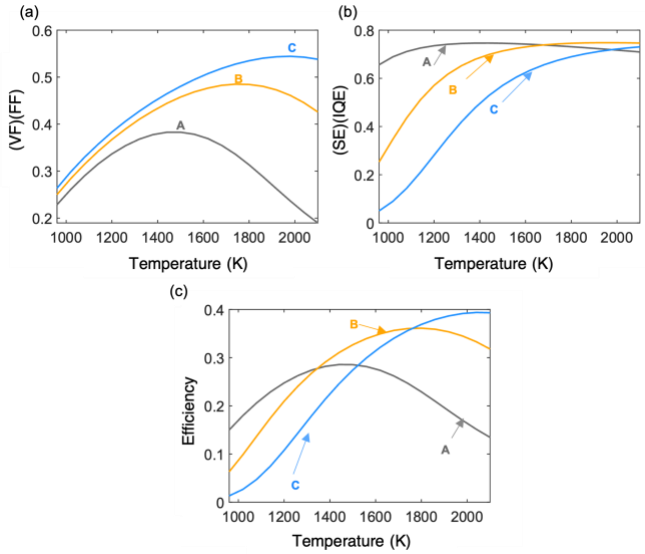

Fig. 2 Carrier management (**a**), spectral management (**b**), and overall TPV efficiency (**c**) as a function of emitter temperature. Device A (grey), B (orange), and C (blue) have bandgaps of 0.74 eV, 1 eV and 1.2 eV respectively.

With regards to spectral management (*SE*)(*IQE*), which depends primarily on R_{out}, the three systems exhibit relatively high and temperature-insensitive performance, as shown in Fig. 2b. We find R_{out} (weighted to a 1700K blackbody emitter) are 98.8%, 99.1% and 99.2% for the 0.74 eV, 1.0 eV and 1.2 eV bandgap cells, respectively. The slight improvement in reflectance with increasing bandgap results since at a constant temperature, there is less power lost to band-edge absorption. We also see that (*SE*)(*IQE*) decreases at lower temperatures, but the onset of this decrease shifts to higher temperatures with increasing bandgap.

Overall, there is a tradeoff between spectral and carrier management for the three different systems, which gives rise to a distinct optimal temperature range for each device. The 0.74 eV device (A) has improved efficiency in the range of 1000 K to 1300 K, making it suitable for applications such as waste heat recovery and concentrated solar thermal. In the moderate temperature range of 1300 K to 1700 K, device B produces the best efficiency, with potential applications in space exploration and distributed cogeneration. Lastly, at >1700 K, device C has the highest conversion efficiency, suitable for applications in thermal energy grid storage. Of note, with these three devices, all with the same architecture and from the same material system, one can achieve near-optimal performance over wide range of emitter temperatures, spanning 1000 to 2200 K.

IV. Experiment

Fig. 3a shows a scanning electron microscopy (SEM) image featuring the airbridge architecture. The emitter used for the testing these device is a Joule-heated graphite felt suspended over the cell. This setup allows us to achieve high emitter temperatures and large view factors using a single configuration. We have demonstrated emitter temperatures up to 2273 K as shown in Fig. 3b. The heat absorbed, Q_{abs}, by these cells can be quantified using a calorimeter consisting of a copper pedestal with embedded temperature measurements that determine the heat flux. Detailed results from these experimental studies will be presented.

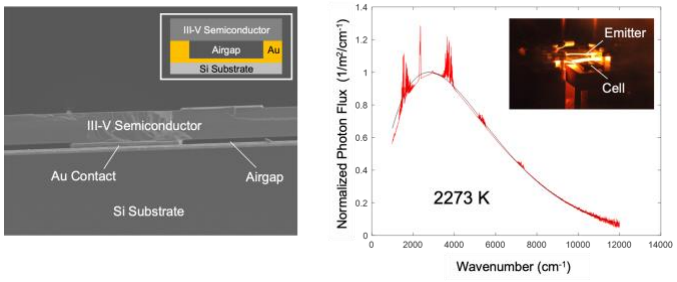

Fig. 3 (**a**) Cross section SEM of the airbridge cell. (**b**) Measured and simulated emission spectra from the graphite felt heater.

V. Conclusion

This work provides insights into how efficiency can be maximized across a wide range of emission temperatures by designing airbridge cells with varying bandgaps within a single lattice-matched material system. Experimental devices and a novel characterization platform are presented to support the theoretical results.

References

[1] A. Lenert, D. M. Bierman, Y. Nam, W. R. Chan, I. Celanovic, and E. N. Wang, "A nanophotonic solar thermophotovoltaic device," *Nat. Nanotechnol.*, vol. 9, no. 2, pp. 126–130, 2014, doi: 10.1038/nnano.2013.286.

[2] A. Datas, A. Ramos, A. Martí, C. del Cañizo, and A. Luque, "Ultra high temperature latent heat energy storage and thermophotovoltaic energy conversion," *Energy*, vol. 107, pp. 542–549, 2016, doi: 10.1016/j.energy.2016.04.048.

[3] A. LaPotin *et al.*, "Thermophotovoltaic efficiency of 40%," *Nature*, vol. 604, no. 7905, pp. 287–291, 2022, doi: 10.1038/s41586-022-04473-y.

[4] L. M. Fraas, J. E. Avery, and H. X. Huang, "Thermophotovoltaic furnace-generator for the home using low bandgap GaSb cells," *Semicond. Sci. Technol.*, vol. 18, no. 5, 2003, doi: 10.1088/0268-1242/18/5/316.

[5] D. Fan, T. Burger, S. Mcsherry, B. Lee, A. Lenert, and S. R. Forrest, "Near-perfect photon utilization in an air-bridge thermophotovoltaic cell," *Nature*, no. February, 2020, doi: 10.1038/s41586-020-2717-7.

[6] Z. Omair, L. M. Pazon-Outon, and E. Yablonovitch, "Practical challenges towards 50% efficient thermophotovoltaic energy conversion," vol. 1112002, no. September 2019, p. 1, 2019, doi: 10.1117/12.2534511.

[7] T. Burger, B. Roy-Layinde, R. Lentz, Z. J. Berquist, S. R. Forrest, and A. Lenert, "Semitransparent thermophotovoltaics for efficient utilization of moderate temperature thermal radiation," *Proc. Natl. Acad. Sci.*, vol. 119, no. 48, p. e2215977119, 2022, doi: 10.1073/pnas.2215977119.

[8] T. Burger, C. Sempere, B. Roy-Layinde, and A. Lenert, "Present Efficiencies and Future Opportunities in Thermophotovoltaics," *Joule*, vol. 4, no. 8, pp. 1660–1680, 2020, doi: 10.1016/j.joule.2020.06.021.

[9] R. L. Moon, G. A. Antypas, and L. W. James, "Bandgap and lattice constant of GaInAsP as a function of alloy composition," *J. Electron. Mater.*, vol. 3, no. 3, pp. 635–644, 1974, doi: 10.1007/BF02655291.

[10] P. Jurczak, A. Onno, K. Sablon, and H. Liu, "Efficiency of GaInAs thermophotovoltaic cells: the effects of incident radiation, light trapping and recombinations," *Opt. Express*, vol. 23, no. 19, p. A1208, Sep. 2015, doi: 10.1364/oe.23.0a1208.

[11] B. Roy-Layinde *et al.*, "Sustaining efficiency at elevated power densities in InGaAs airbridge thermophotovoltaic cells," *Sol. Energy Mater. Sol. Cells*, vol. 236, no. December 2021, p. 111523, 2022, doi: 10.1016/j.solmat.2021.111523.

[12] T. Burger, D. Fan, K. Lee, S. R. Forrest, and A. Lenert, "Thin-Film Architectures with High Spectral Selectivity for Thermophotovoltaic Cells," *ACS Photonics*, vol. 5, no. 7, 2018, doi: 10.1021/acsphotonics.8b00508.